Electronic Supplementary Information (ESI)

Silver(I) *N*-heterocyclic carbene complexes are potent uncompetitive inhibitors of the papain-like protease with antiviral activity against SARS-CoV-2

Maria Gil-Moles [a,b], Cillian O'Beirne [a], Igor V. Esarev [a], Petra Lippmann [a], Matthias Tacke [c], Jindrich Cinatl [d], Denisa Bojkova [d], Ingo Ott [a]*

a) Institute of Medicinal and Pharmaceutical Chemistry, Technische Universität Braunschweig, Beethovenstr. 55, 38106 Braunschweig, Germany
b) Departamento de Química, Universidad de La Rioja, Centro de Investigación de Síntesis Química (CISQ), Complejo Científico Tecnológico, 26004 Logroño, Spain
c) School of Chemistry, University College Dublin, Belfield, Dublin 4, Ireland
d) Institute of Medical Virology, Universitätsklinikum Frankfurt, Paul-Ehrlich-Str. 40, 60596 Frankfurt, Germany

Table of Contents

1) Comparison of the C2 signal shifts in the ^{13}C-NMR spectra

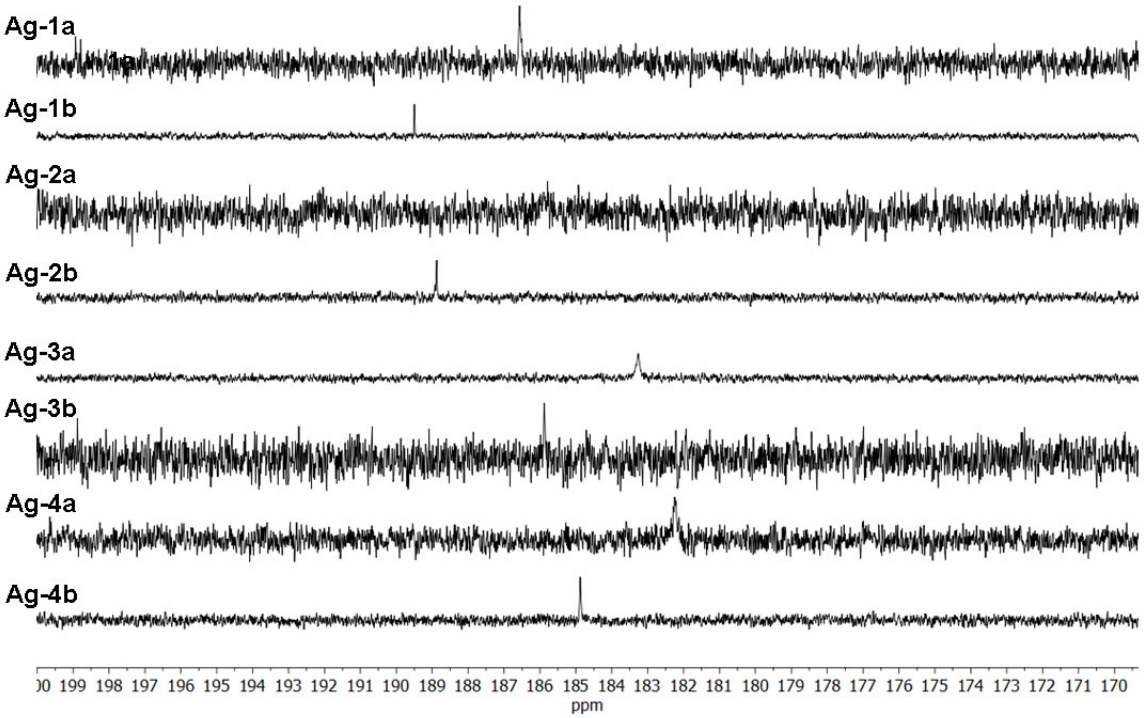

Figure S1: ^{13}C-NMR (DMSO, 126 Mhz) of silver complexes **1a/b** to **4a/b** in the region of 199-171 ppm showing the C2 carbon signals,

2) ^{109}Ag-NMR spectra for Ag-4a and Ag-4b

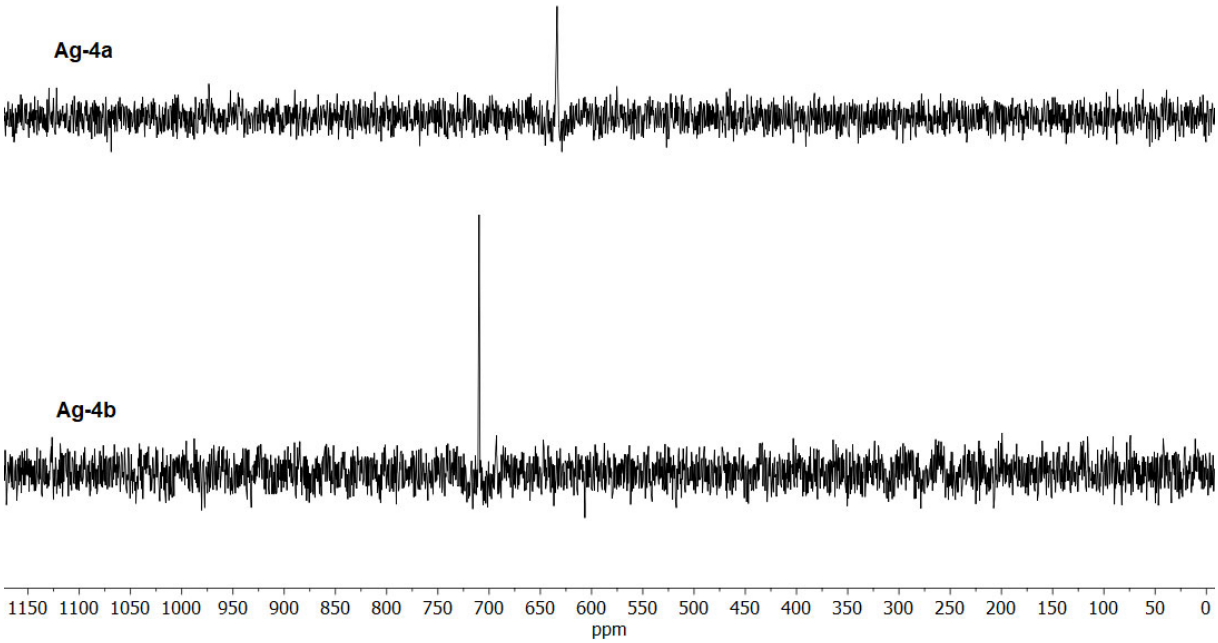

Figure S2: ^{109}Ag-NMR (DMSO, 13.97 MHz) of silver complexes **Ag-4a** and **Ag-4b**.

3) Conductometry experiments in diluted solutions

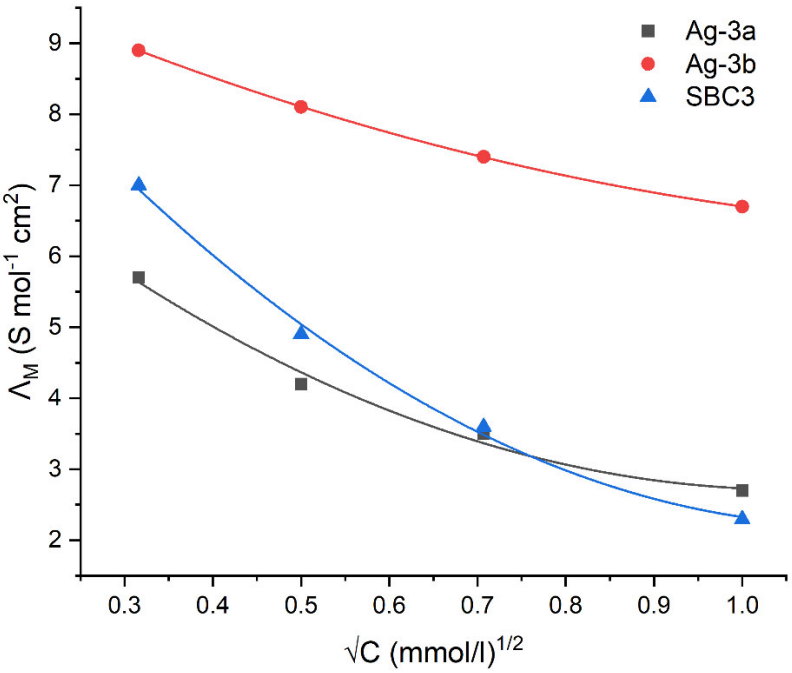

Figure S3: Conductivity Λ_M, Smol^{-1}cm^2 in 0.1 to 1.0 mM solutions in DMSO. The concentration is expressed as square root

4) Time dependent inhibition of SARS-CoV-2 PL^{pro}

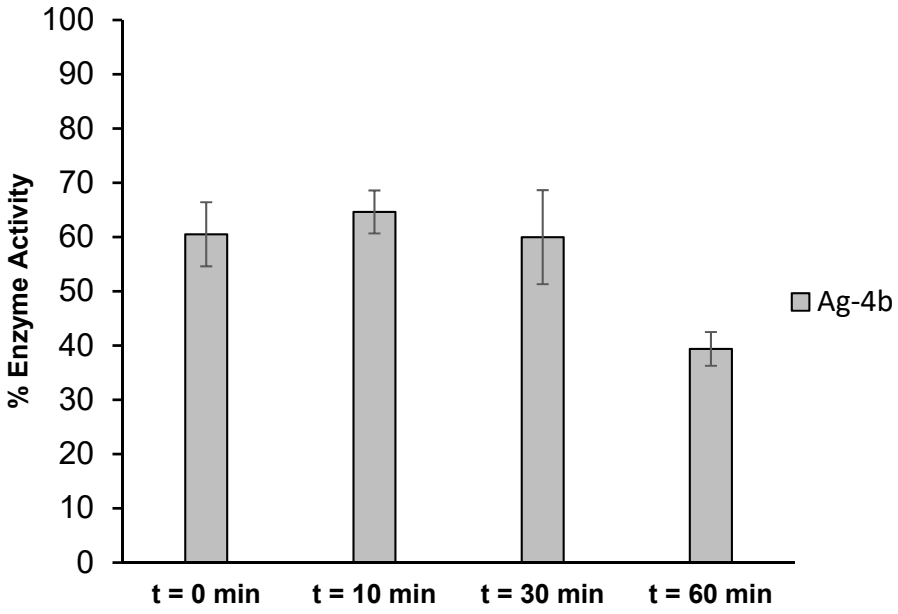

Figure S4: SARS-CoV-2 enzymatic activity after exposure to 0.75 µM of **Ag-4b** for 0 to 60 minutes (n=2).

5) Enzyme kinetics for inhibition of SARS-CoV-2 by Ag-4b

A kinetic study was performed, to determine important parameters such as V_{max} (maximum velocity of enzymatic reaction) and K_m (interaction constant between enzyme and substrate/Michaelis Menten constant). These parameters undergo changes in the absence and presence of different concentrations of inhibitor. These changes allow to evaluate which mechanism of inhibition occurs. Therefore, the experiment was carried out using a constant enzyme concentration (0.2 μM) and different concentrations of inhibitor **Ag-4b** (0, 0.1, 0.25 and 0.75 μM). The mixture was incubated for 10 min at 37 ºC. After the incubation period, different substrate concentrations were added in the range of 10-4000 μM and the fluorescence emission was measured immediately every minute for 1 h (λ_{exc}=355 nm; λ_{em}=460 nm) at 37 °C. Initially the product is formed in a linear manner over time and the slope of thereof corresponds to the velocity of the enzymatic reaction at a certain concentration of substrate (V). As an example, figure S4 top shows the amount of product obtained versus time for the following conditions: [E] = 0.2 μM, [I] = 0 μM, [S] = 1000 μM (only one graph is shown for simplicity). Hence, from these data a new graph can be generated (see red marks in figure S4), according to the Michaelis Menten model (see equation 1) representing velocity (V, mol product/time) versus substrate concentration ([S], μM). With this graph (see figureS4 bottom) the values of V_{max} and K_m can be obtained, where V_{max} is the highest point on the Y-axis and $V_{max}/2$ is correlated with K_m (see figure S4 bottom, for clarity, only V_{max} and K_m have been marked on the graph obtained with [I] = 0.1 μM.) In addition, in figure S4 bottom it could also be noted that the velocity (V) increases with increasing concentration of substrate [S] until 1000 μM. Above this concentration, the substrate itself acts as an inhibitor, such behaviour has been previously described (see scheme S1) [1].

$$V = \frac{V_{max}[S]}{k_m + [S]} \quad (1)$$

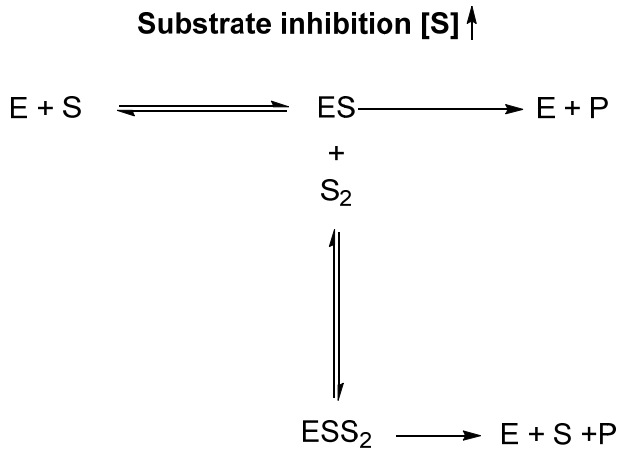

Scheme 1: Reaction between enzyme "E" and substrate "S" at high substrate concentrations

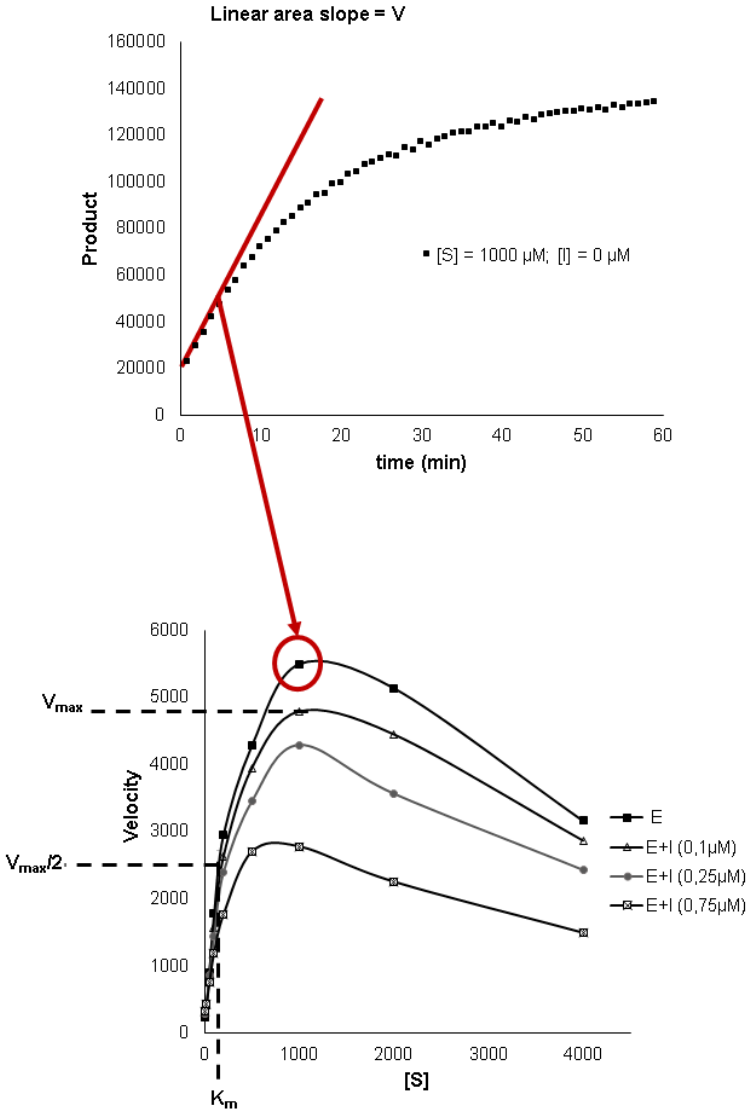

Figure S5: (Top) product vs time, where the slope of the linear range corresponds to the velocity. (Bottom) velocity "V" vs substrate concentration [S], where V_{max} is the maximum velocity of enzymatic reaction and K_m is the Michaelis Menten constant.

To determine the mechanism of inhibition and calculate more accurately V_{max} and K_m the Lineweaver-Burke equation was necessary (equation 2). This representation gives a linear regression (see figure S5) where the slope is K_m/V_{max}, the intersection with the Y-axis corresponds to $1/V_{max}$ and intersection with the X-axis corresponds to $-1/K_m$. Figure S5 shows the typical behaviour for an uncompetitive inhibitor, since increasing the concentration of **Ag-4b** results in parallel lines and this is translated into both V_{max} and K_m decreasing. An uncompetitive inhibitor interacts only with the enzyme-substrate complex and therefore the binding of the inhibitor is promoted for the presence of the substrate (see figure S6 right)[1] Table S1 shows the values obtained for V_{max} and K_m as well as the slope values (K_m/V_{max}) for each case ([I] = 0, 0.1, 0.25, 0.75 µM).

$$\frac{1}{V} = \frac{k_m}{V_{max}} \frac{1}{[S]} + \frac{1}{V_{max}} \quad (2)$$

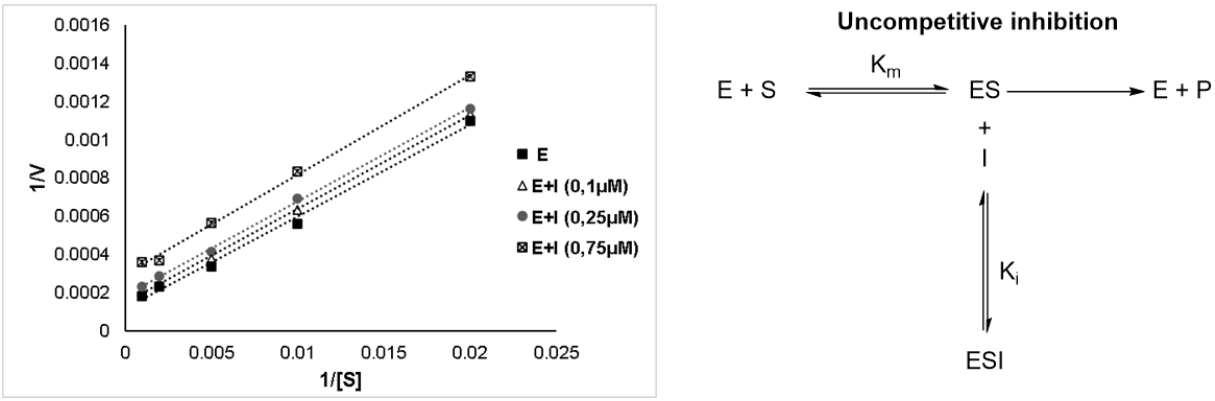

Figure S6: Lineweaver-Burke graph (left), scheme of reaction (right).

Table S1: Kinetics parameters in absence and in presence of different concentrations of inhibitor (**Ag-4b**).

	K_m	K_i	V_{max}	K_m/V_{max}
E	411	-	8547	0.050 ± 0.002
E + I 0.1 µM	328	0.48 ± 0.22	6667	
E + I 0.25 µM	264		5376	
E + I 0.75 µM	176		3378	

Taking the reaction scheme of an uncompetitive inhibitor into account, it was possible to calculate the interaction constant between the enzyme-substrate-inhibitor complex "ESI" (K_i). Equation 3 shows the relationship between V, V_{max}, K_m and K_i with V, V_{max} and K_m being known values for the different concentrations of [I] and [S] and allows calculation of K_i

(equation 3.1). As shown in table 1, $K_i = 0.48 \pm 0.22$ indicating that the affinity shown by the inhibitor for the enzyme-substrate complex is four orders of magnitude higher than the affinity between enzyme and substrate.

$$V = \frac{V_{max}[S]}{[S]\left(1 + \frac{[I]}{K_i}\right) + K_m} \quad (3) \qquad K_i = \frac{V[S][I]}{[S]V_{max} - V[S] - VK_m} \quad (3.1)$$

[1] Enzymes as drug targets. In Pharmacology in Drug Discovery and Development (pp.131-156), DOI 10.1016/B978-0-12-803752-2.00006-5.

6) Toxicity of silver NHC complexes against Caco-2 cells

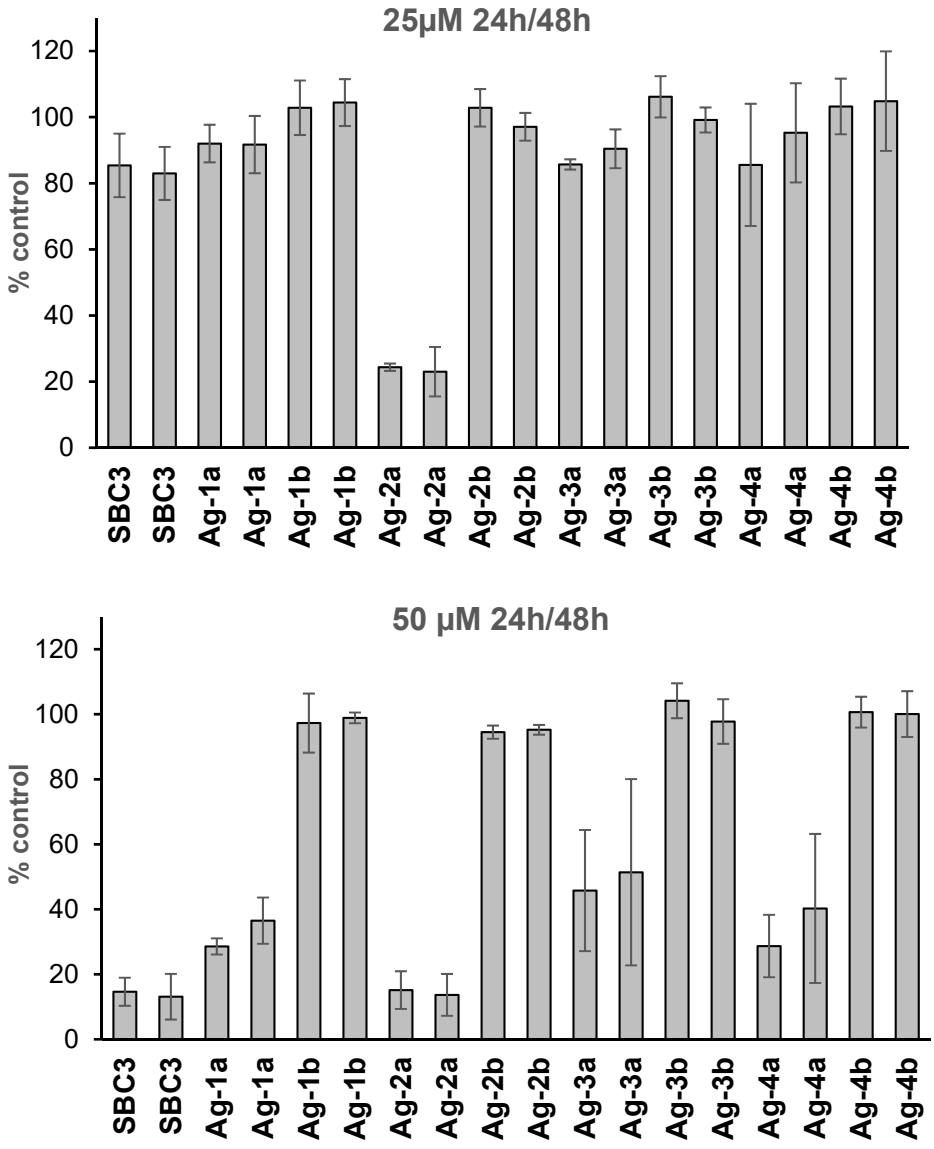

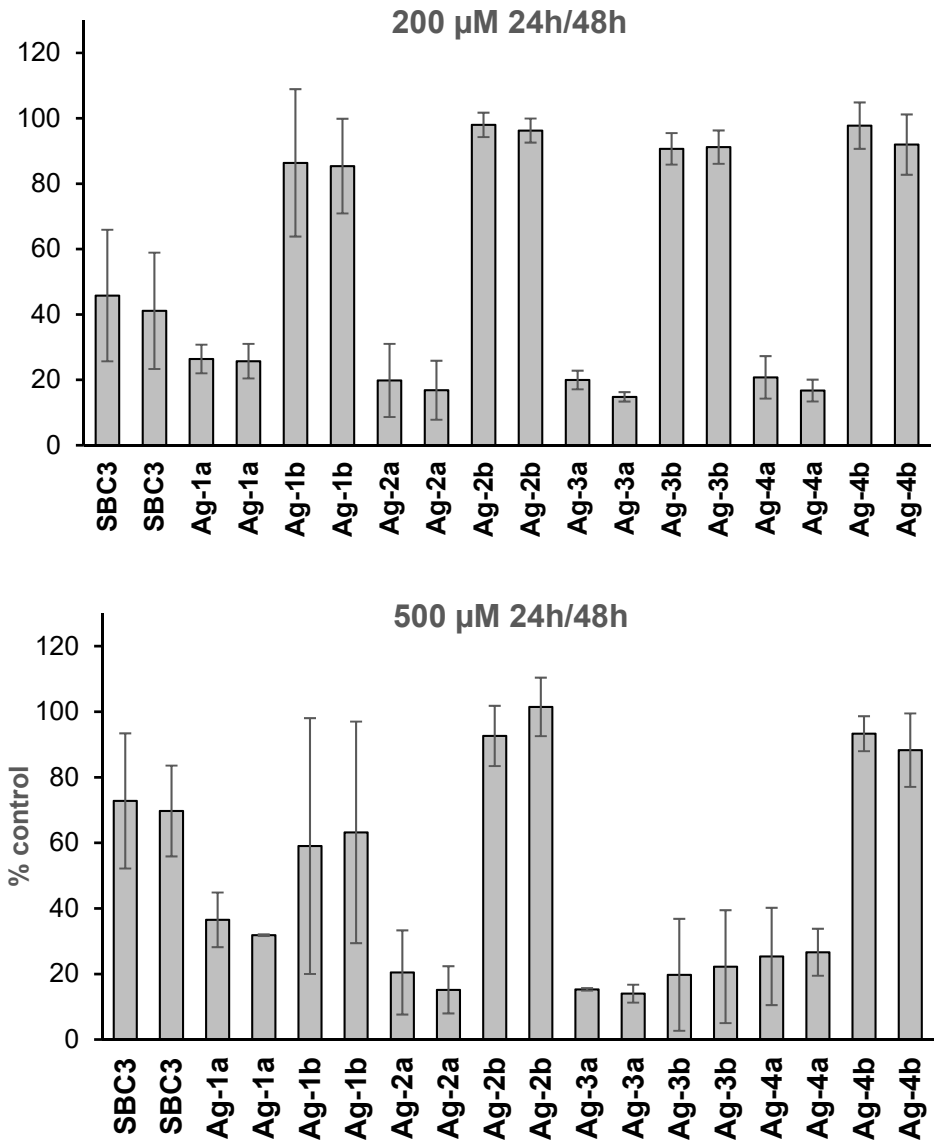

Figure S7: Cytotoxicity of 25, 50, 200 and 500 µM of silver NHC complexes against almost confluent cell layers of Caco-2 cells (as % control of untreated cells). left bars: 24h, right bars: 48h.

7) ^{1}H-NMR and ^{13}C-NMR spectra of silver complexes 1a/b to 4a/b

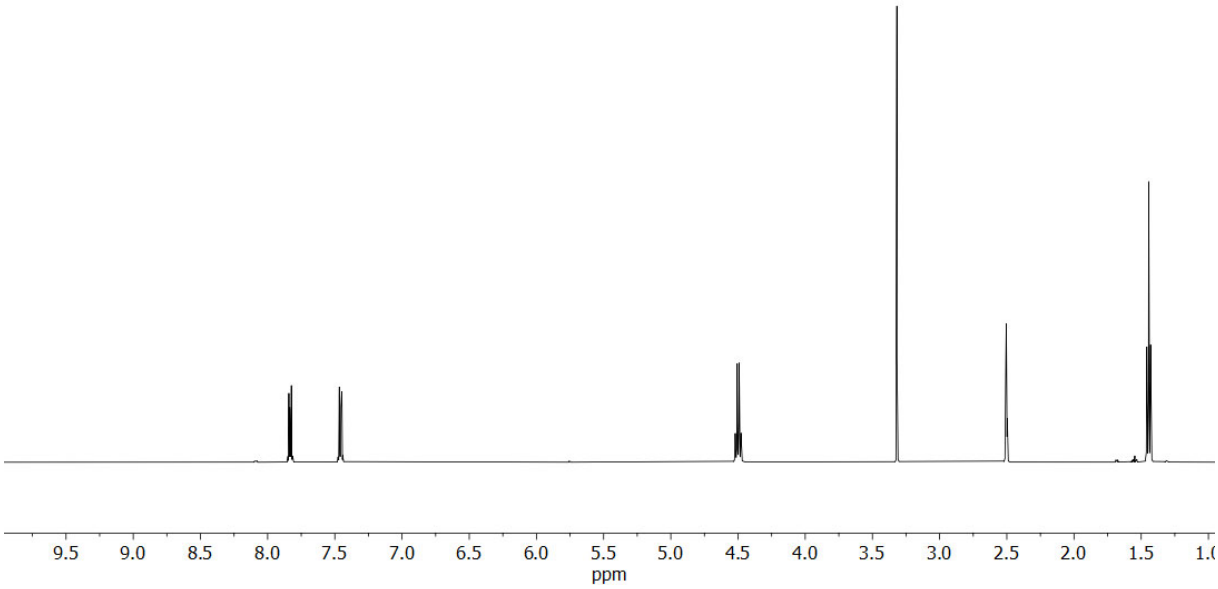

Figure S8: **Ag-1a**, ^{1}H NMR (DMSO, 500 MHz): 7.83 (m, 2H, ArH), 7.46 (m, 2H, ArH), 4.50 (q, 4H, J = 7.3 Hz, 2x CH_2), 1.44 (t, 6H, J = 7.3 Hz, 2x CH_3).

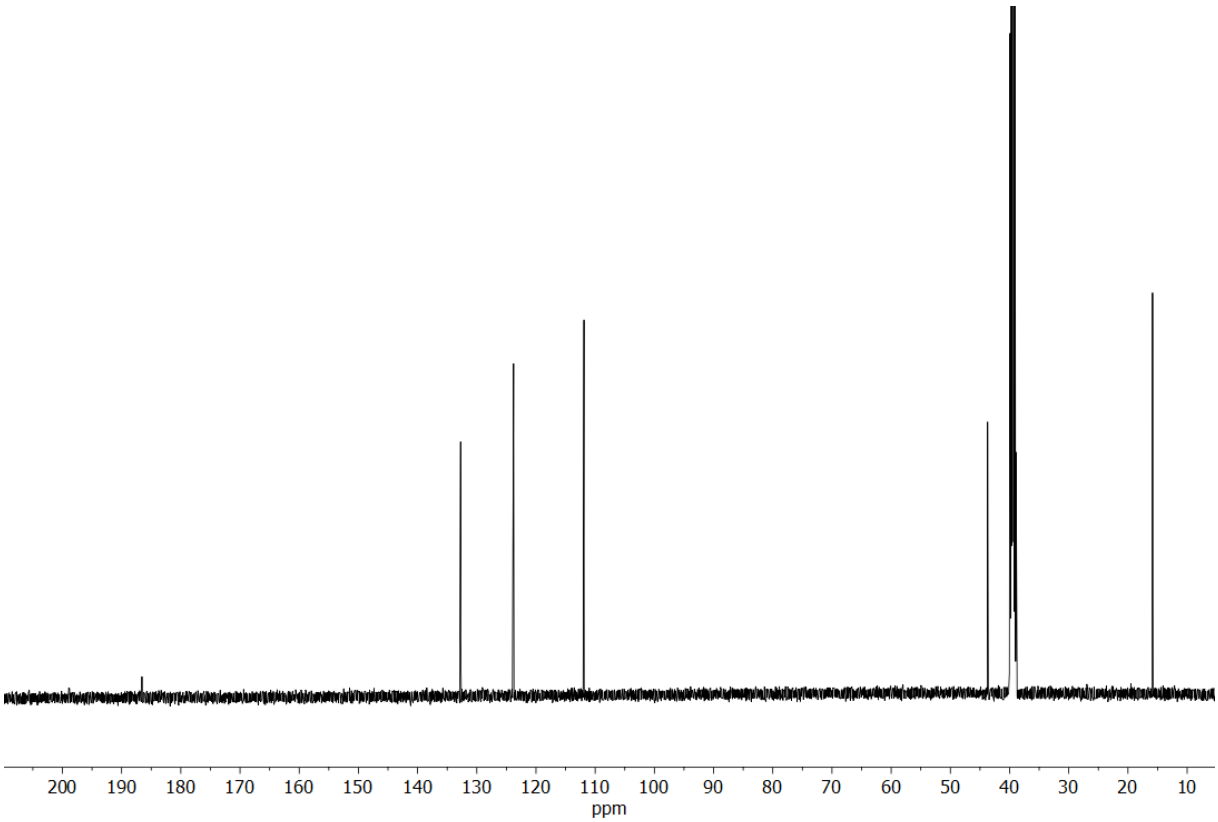

Figure S9: **Ag-1a**, ^{13}C NMR (DMSO, 126 MHz): 186.5 (ArC2), 132.5 (ArC3), 123.7 (ArC), 111.5 (ArC), 43.7 (CH_2), 15.7 (CH_3).

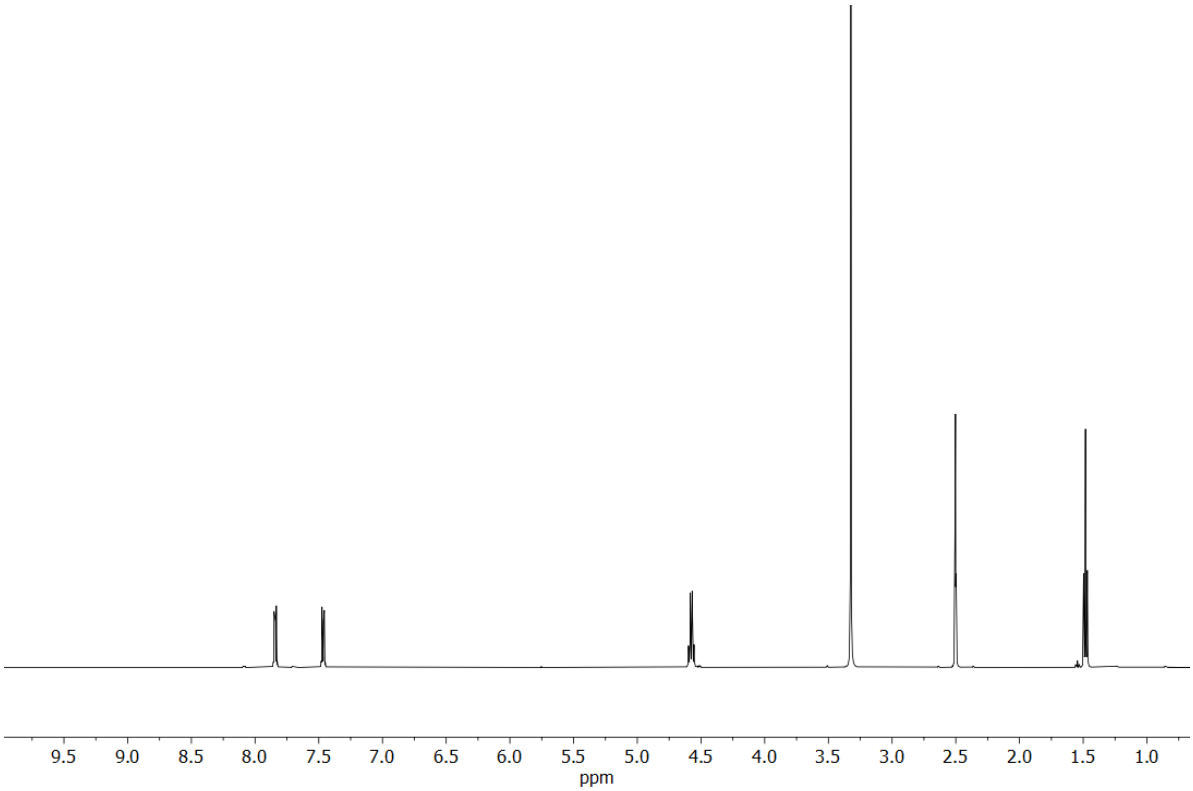

FigureS10: **Ag-1b**, ^{1}H NMR (DMSO, 500 MHz): 7.84 (s, 2H, ArH), 7.47 (m, 2H, ArH), 4.57 (q, 4H, J = 7.2 Hz, 2x CH_2), 1.48 (t, 6H, J = 7.2 Hz, 2x CH_3).

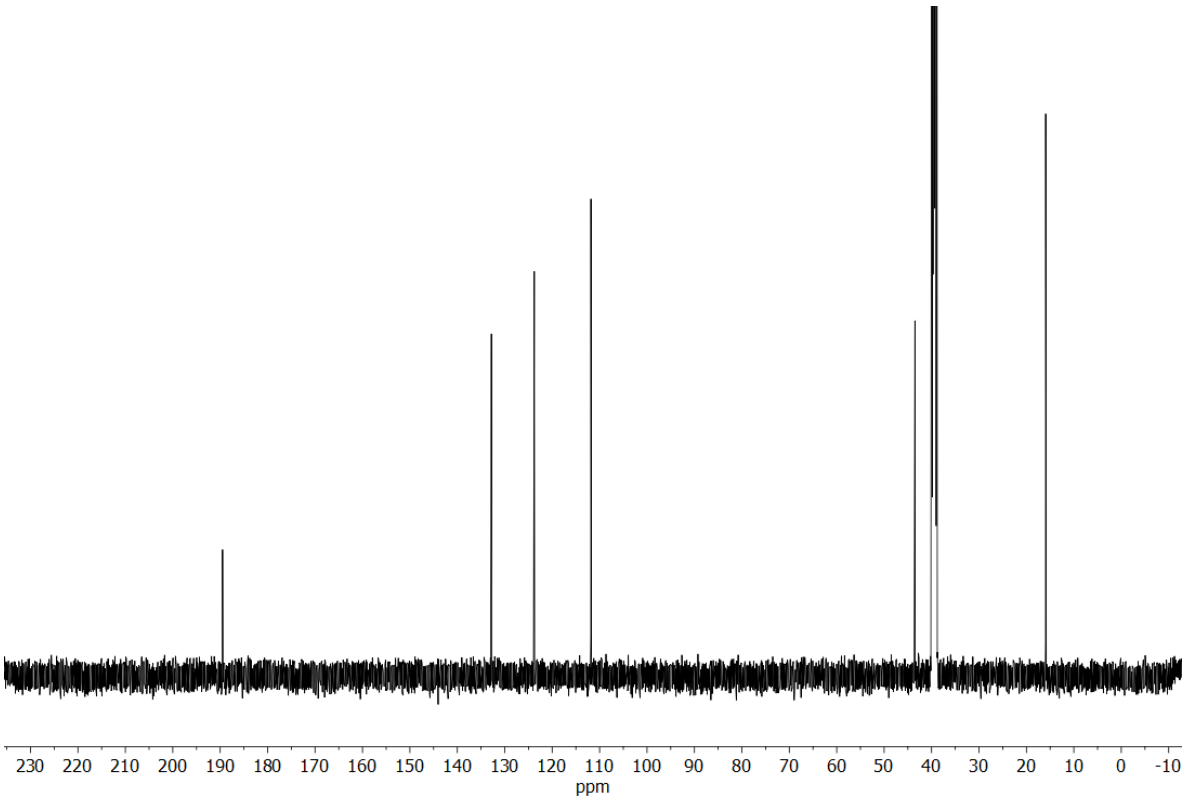

FigureS11: **Ag-1b**, ^{13}C NMR (DMSO, 126 MHz): 189.5 (ArC2), 132.8 (ArC3), 123.7 (ArC), 111.8 (ArC), 43.5 (CH_2), 15.9 (CH_3).

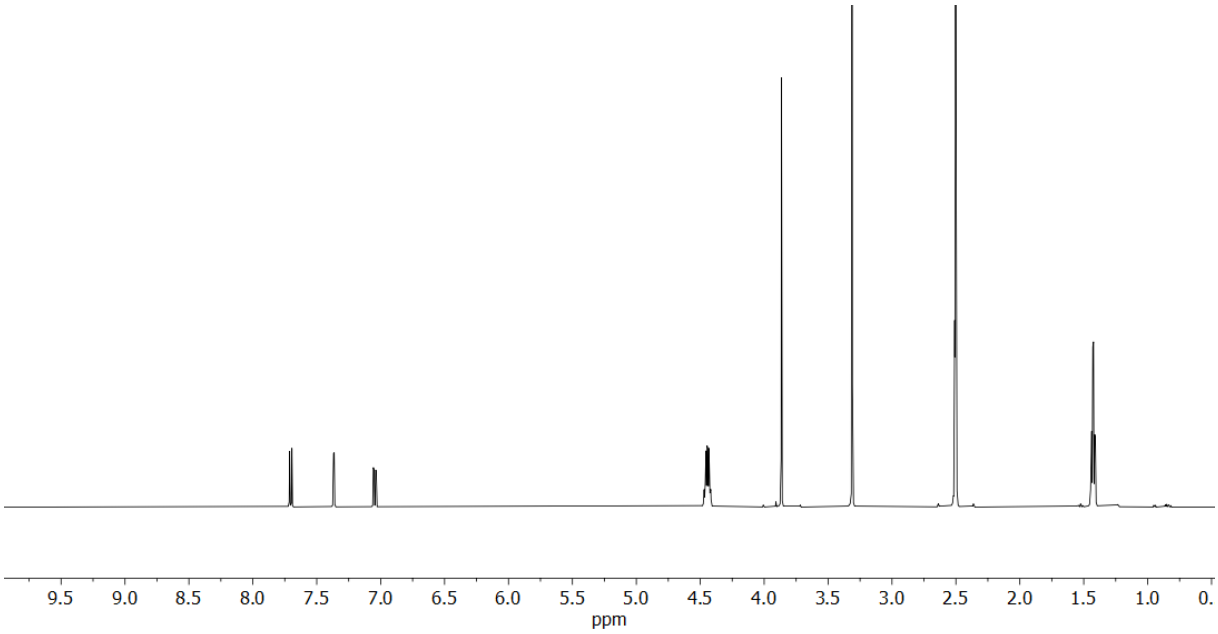

FigureS12: **Ag-2a**, ^{1}H NMR (DMSO, 500 MHz) 7.7 (d, 1H, *J* = 9.1 Hz, ArH7), 7.3 (d, 1H, *J* = 2.3 Hz, ArH4), 7.06 (dd, 1H, *J* = 9.1, 2.3 Hz, ArH6), 4.62 (m, 4H, 2x CH_2), 3.93 (s, 3H, OCH_3), 1.69 (m, 6H, 2x CH_3).

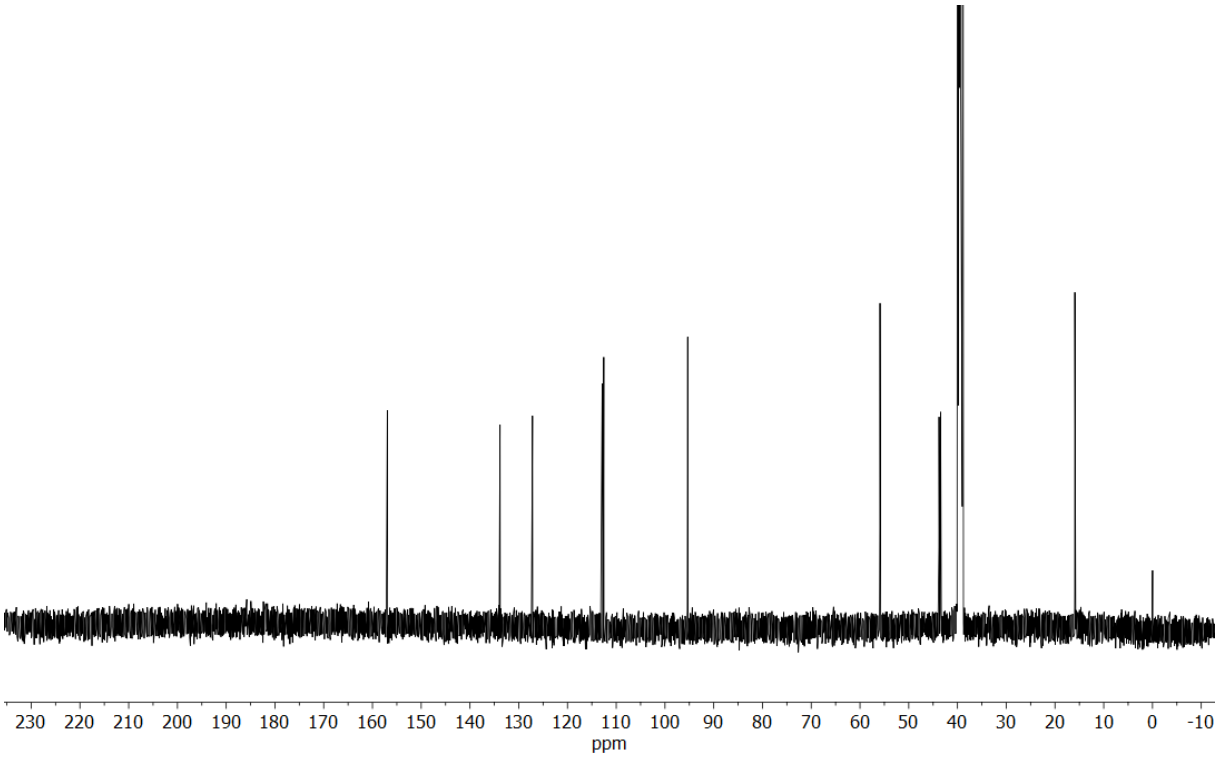

Figure S13: **Ag-2a**, ^{13}C NMR (DMSO, 126 MHz): C2 not detected, 156.8 (ArC5), 133.7 + 127.0 (ArC3 + ArC8), 112.9 (ArC), 112.6 (ArC), 95.3 (ArC), 55.8 (OCH_3), 43.8 (CH_2), 43.4 (CH_2), 15.9 (CH_3), 15.8 (CH_3).

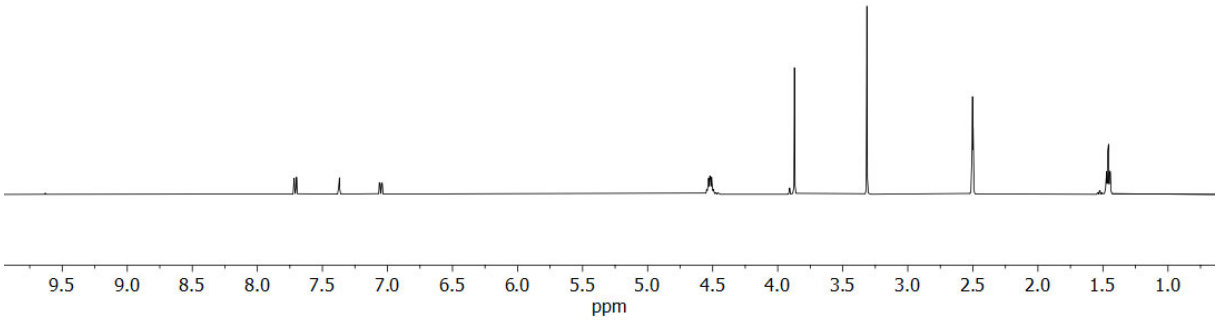

FigureS14: **Ag-2b**, ^{1}H NMR (DMSO, 500 MHz): 7.71 (d, 1H, *J* = 8.9 Hz, ArH7), 7.37 (d, 1H, J = 2.3 Hz, ArH4), 7.05 (dd, 1H, *J* = 8.9, 2.3 Hz, ArH6), 4.51 (m, 4H, 2x CH_2), 3.87 (s, 3H, OCH_3), 1.46 (m, 6H, 2x CH_3).

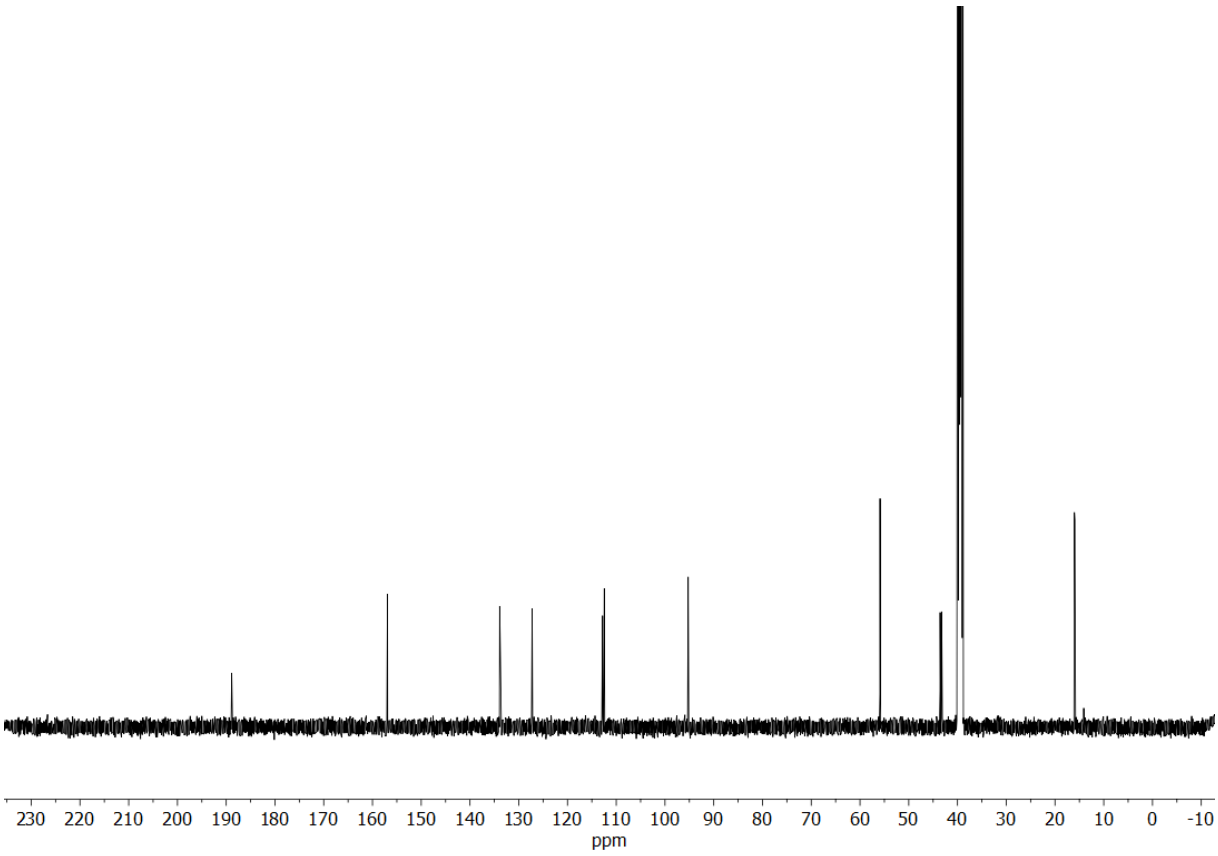

FigureS15: **Ag-2b**, ^{13}C NMR (DMSO, 126 MHz): 188.8 (ArC2), 156.9 (ArC5), 133.9 +127.5 (ArC3 + ArC8), 112.8 (ArC), 112.45 (ArC), 95.2 (ArC), 55.8 (OCH_3), 43.5 (CH_2), 43.2 (CH_2), 16.0 (CH_3), 15.9 (CH_3).

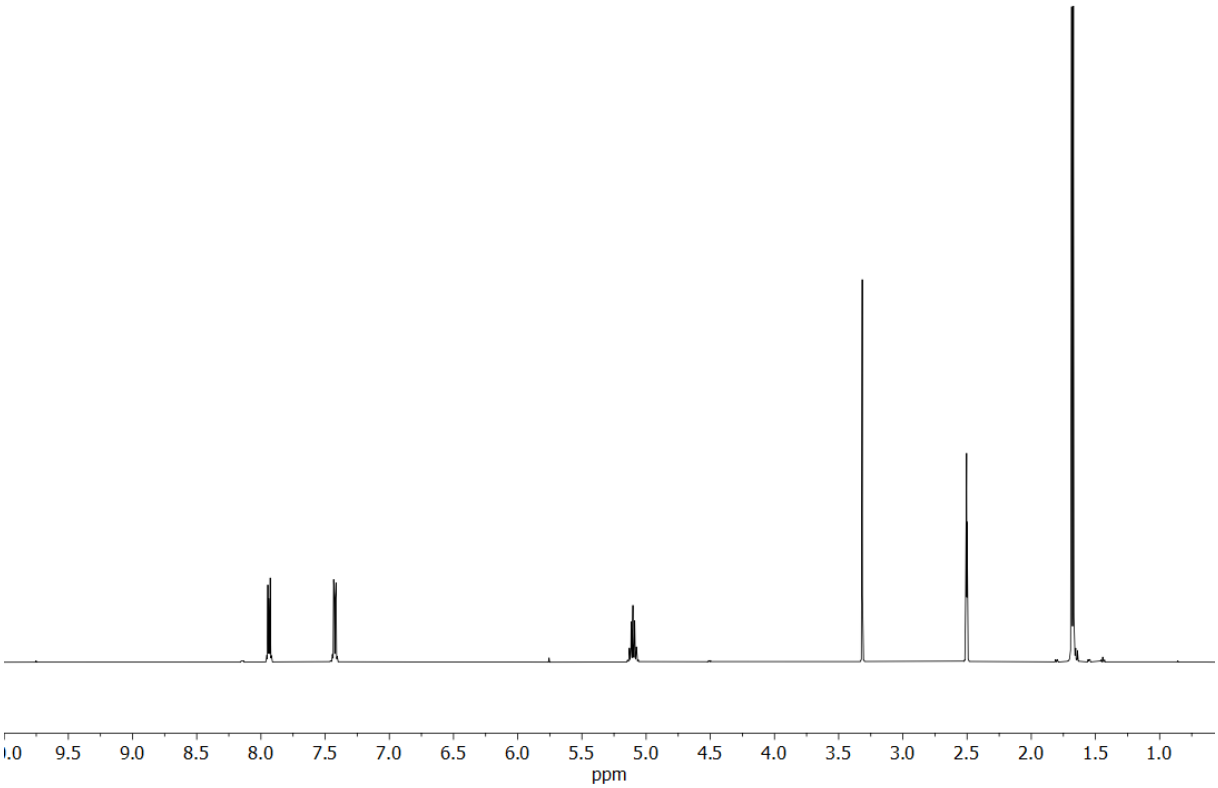

Figure S16: **Ag-3a**, ^{1}H NMR (DMSO, 500 MHz): 7.93 (m, 2H, ArH), 7.42 (m, 2H, ArH), 5.10 (hept, 2H, *J* = 6.9 Hz, 2x CH), 1.67 (d, 12H, J = 6.9 Hz, 2x CH_3).

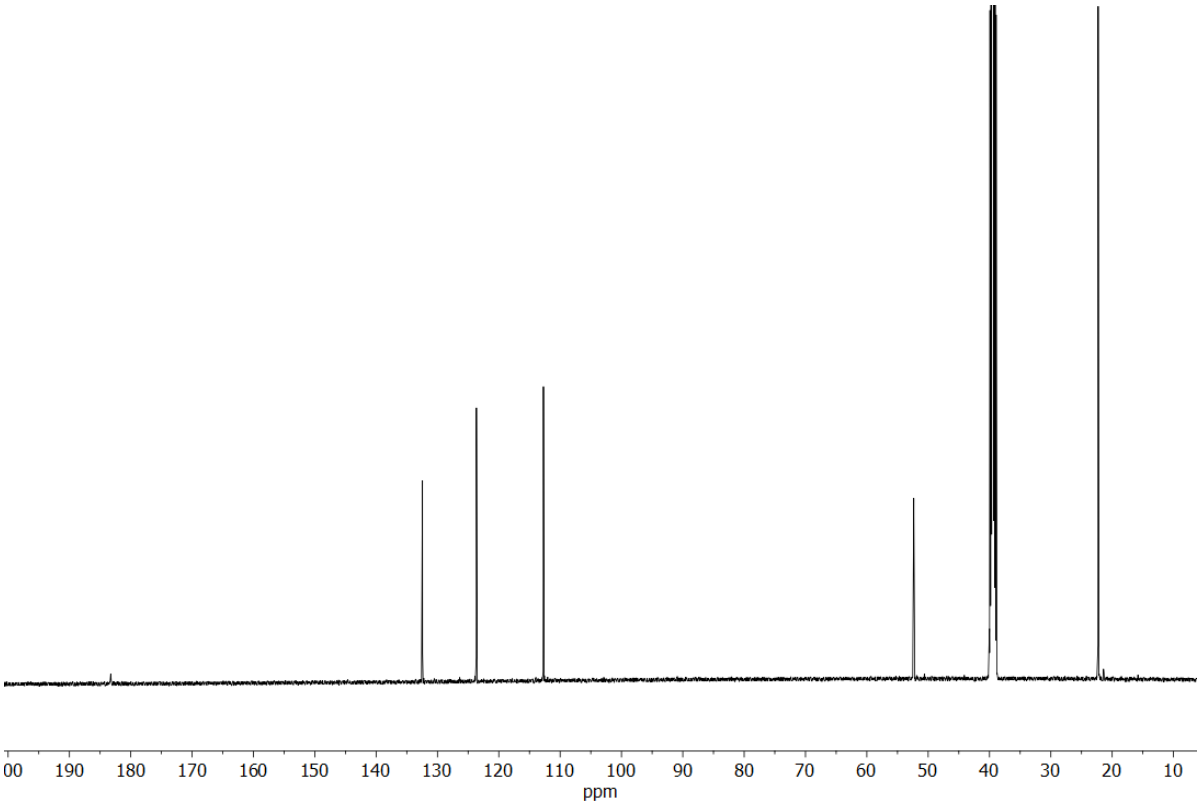

Figure S17: **Ag-3a**, ^{13}C NMR (DMSO, 126 MHz): 183.2 (ArC2), 132.4 (ArC3), 123.6 (ArC), 112.7 (ArC), 52.3 (CH), 22.2 (CH_3).

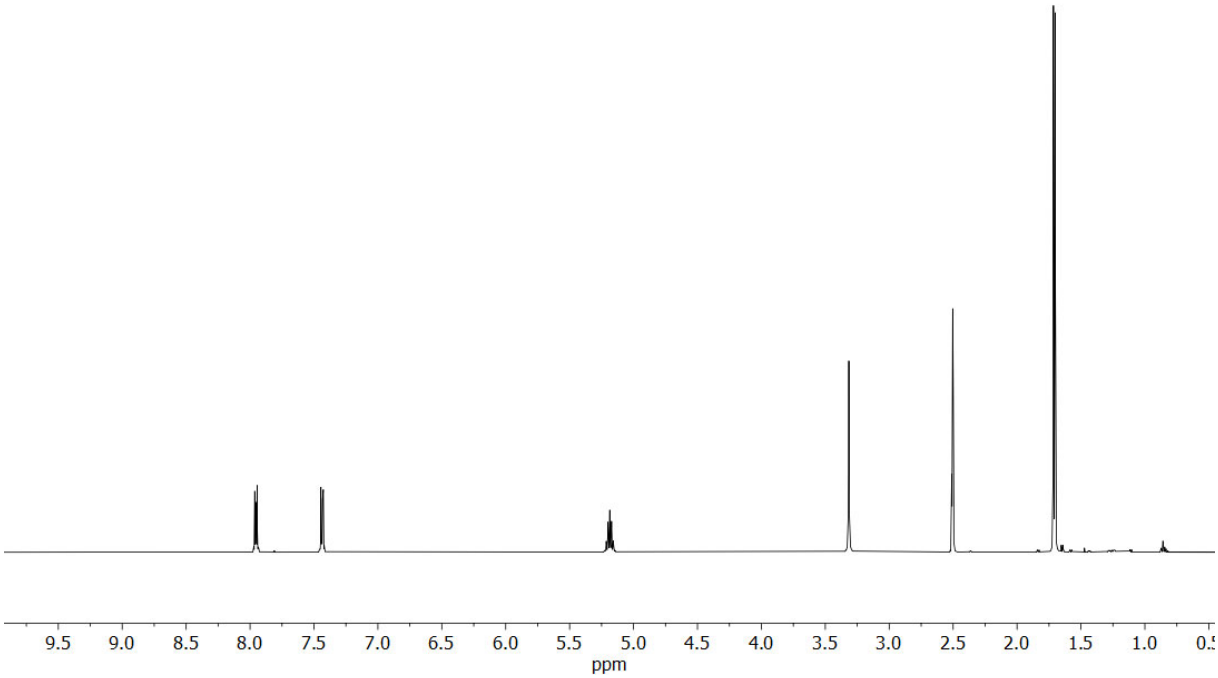

FigureS18: **Ag-3b**, ^{1}H NMR (DMSO, 500 MHz): 7.95 (m, 2H, ArH), 7.44 (m, 2H, ArH), 5.18 (hept, 2H, *J* = 7.0 Hz, 2x CH), 1.71 (d, 12H, J = 7.0 Hz, 4x CH_3.

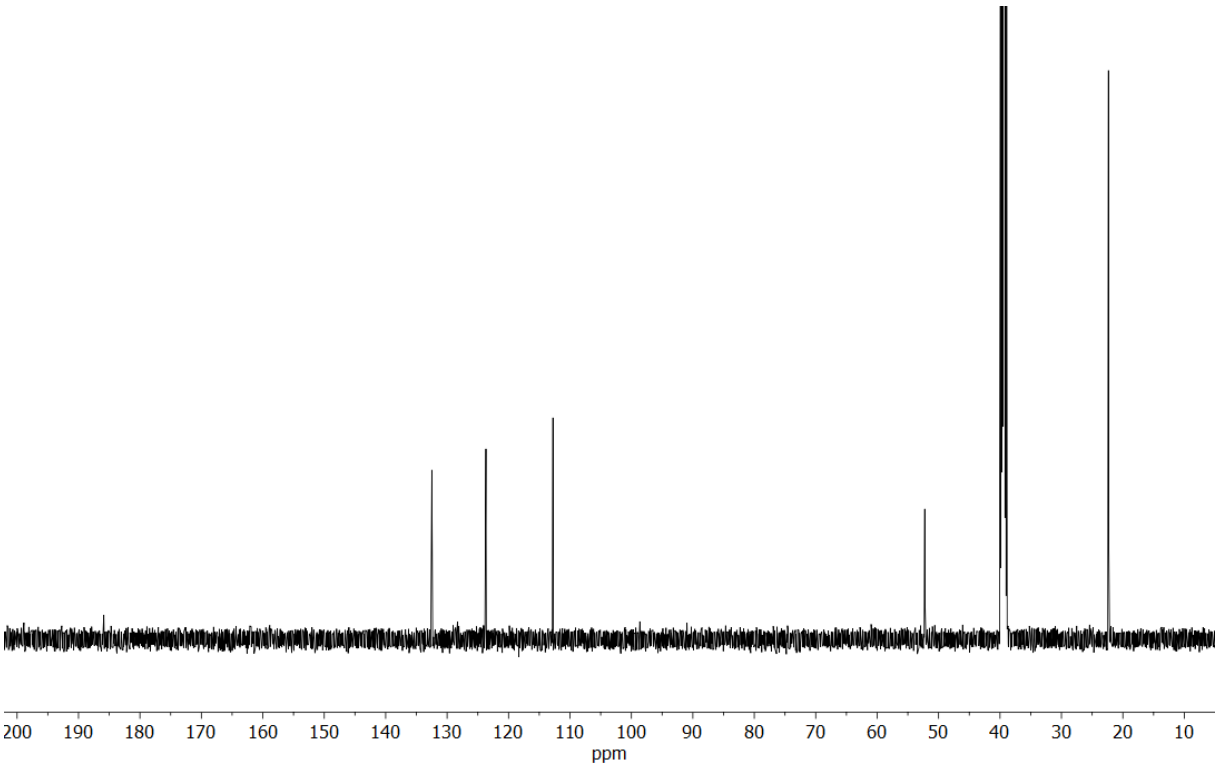

FigureS19: **Ag-3b**, ^{13}C NMR (DMSO, 126 MHZ): 185.8 (ArC2), 132.4 (ArC3), 123.6 (ArC), 112.7 (ArC), 52.2 (CH), 22.3 (CH_3).

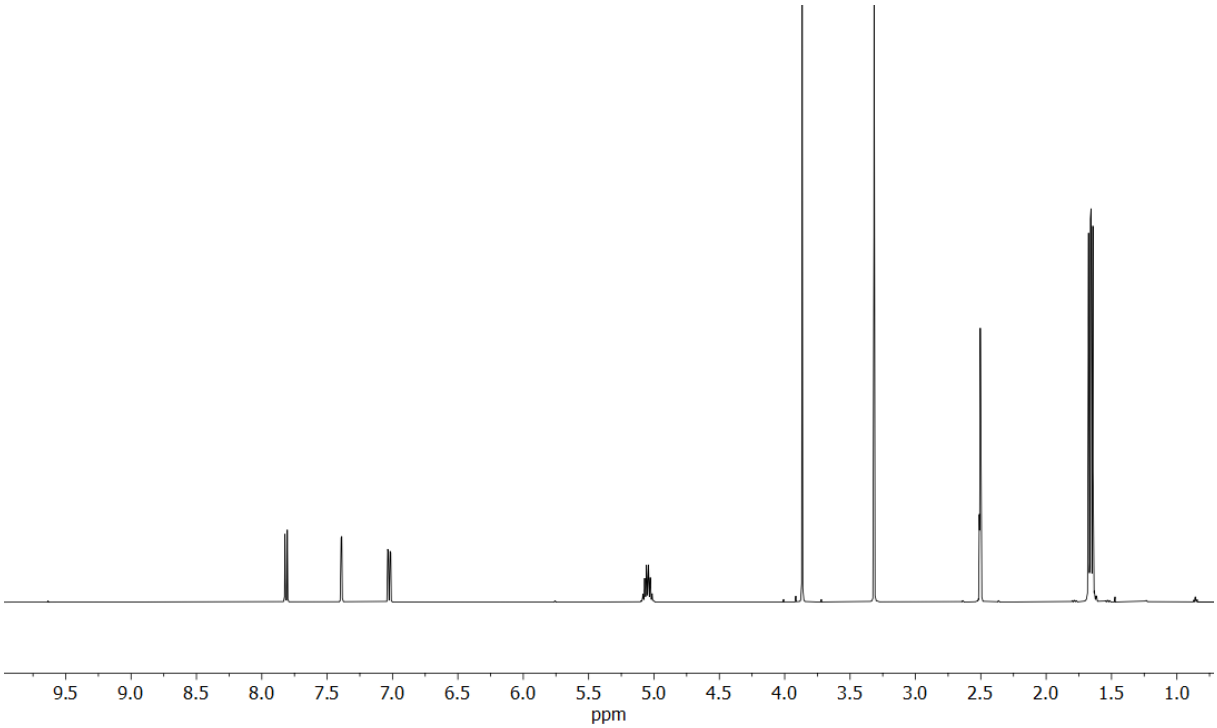

Figure S20: **Ag-4a**, ^{1}H NMR (DMSO, 500 MHz): 7.80 (d, 1H, *J* = 9.0 Hz, ArH7), 7.39 (d, 1H, *J* = 2.3 Hz, ArH4), 7.02 (dd, 1H, *J* = 9.0, 2.3 Hz, ArH6), 5.04 (m, 2H, 2x CH), 3.31 (s, 3H, OCH_3), 1.66 (m, 12H, CH_3).

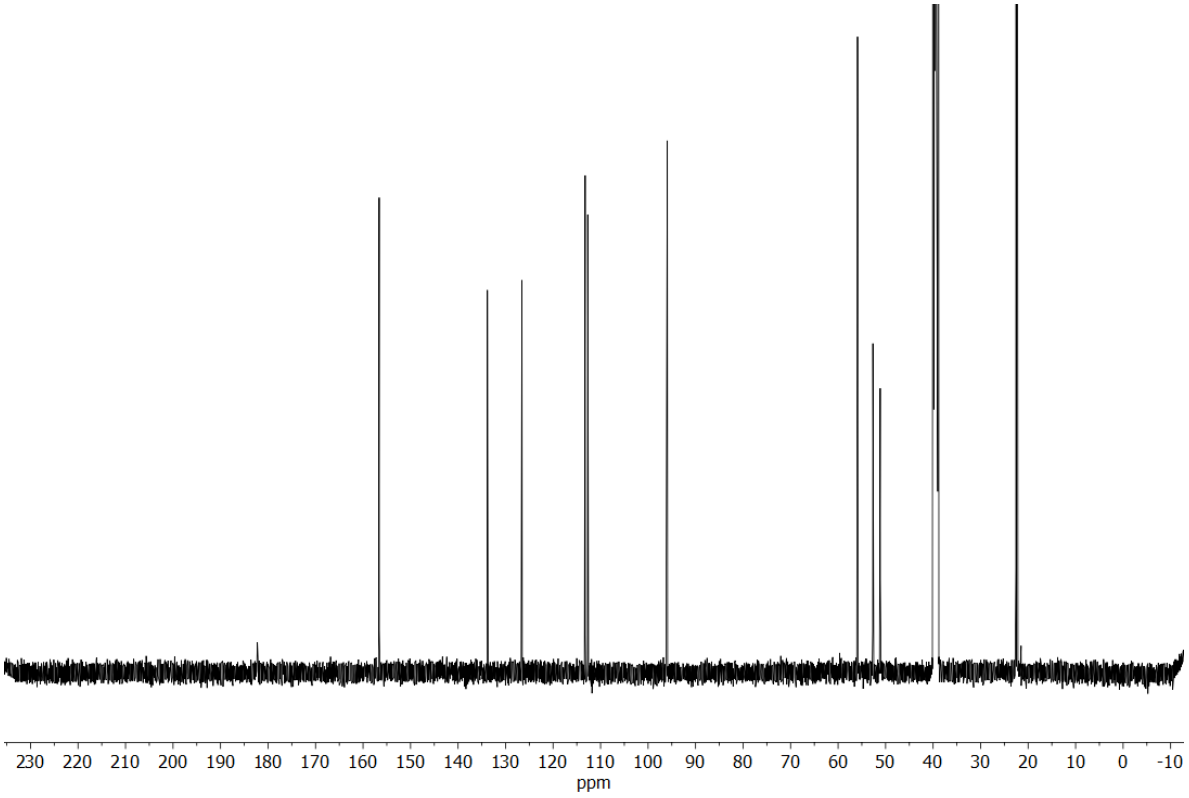

Figure S21: **Ag-4a**, ^{13}C NMR (DMSO, 126 MHz): 182.0 (ArC2), 156.4 (ArC5), 133.7 + 126.5 (ArC3 + ArC8), 113.3(ArC), 112.5 (ArC), 95.6 (ArC), 55.6 (OCH_3), 52.6 (CH), 51.0 (CH), 22.5 (CH_3), 22.3 (CH_3)

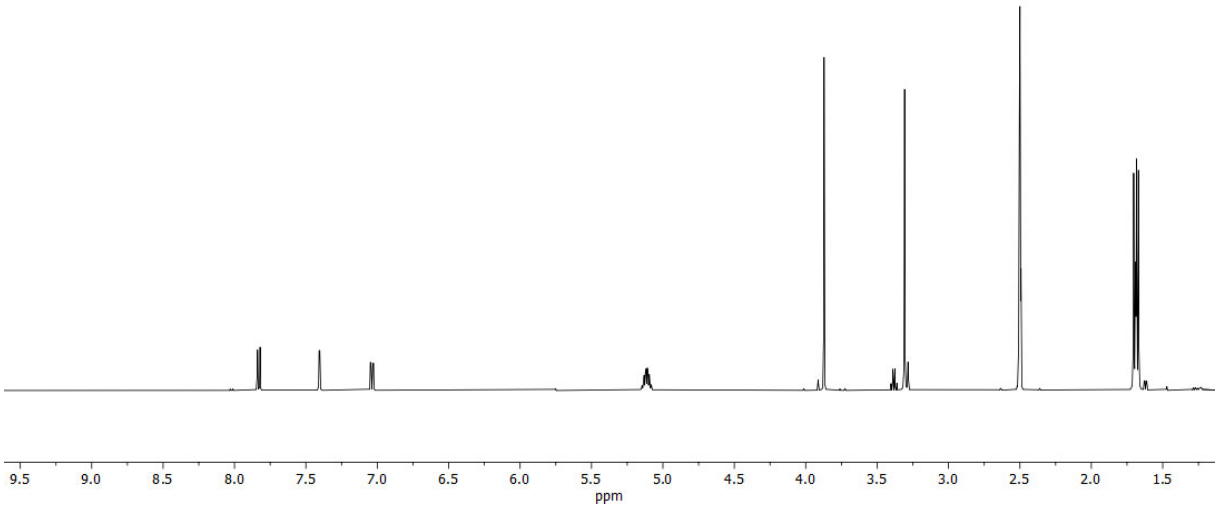

Figure S22: **Ag-4b**, ^{1}H NMR (DMSO, 500 MHz): 7.81 (d, 1H, *J* = 8.7 Hz, ArH7), 7.40 (d, 1H, *J* = 2.4 Hz, ArH4), 7.03 (dd, 1H, *J* = 8.7, 2.4 Hz, ArH6), 5.11 (m, 2H, 2x CH), 3.87 (s, 3H, OCH_3), 1.68 (m, 12H, 4x CH_3).

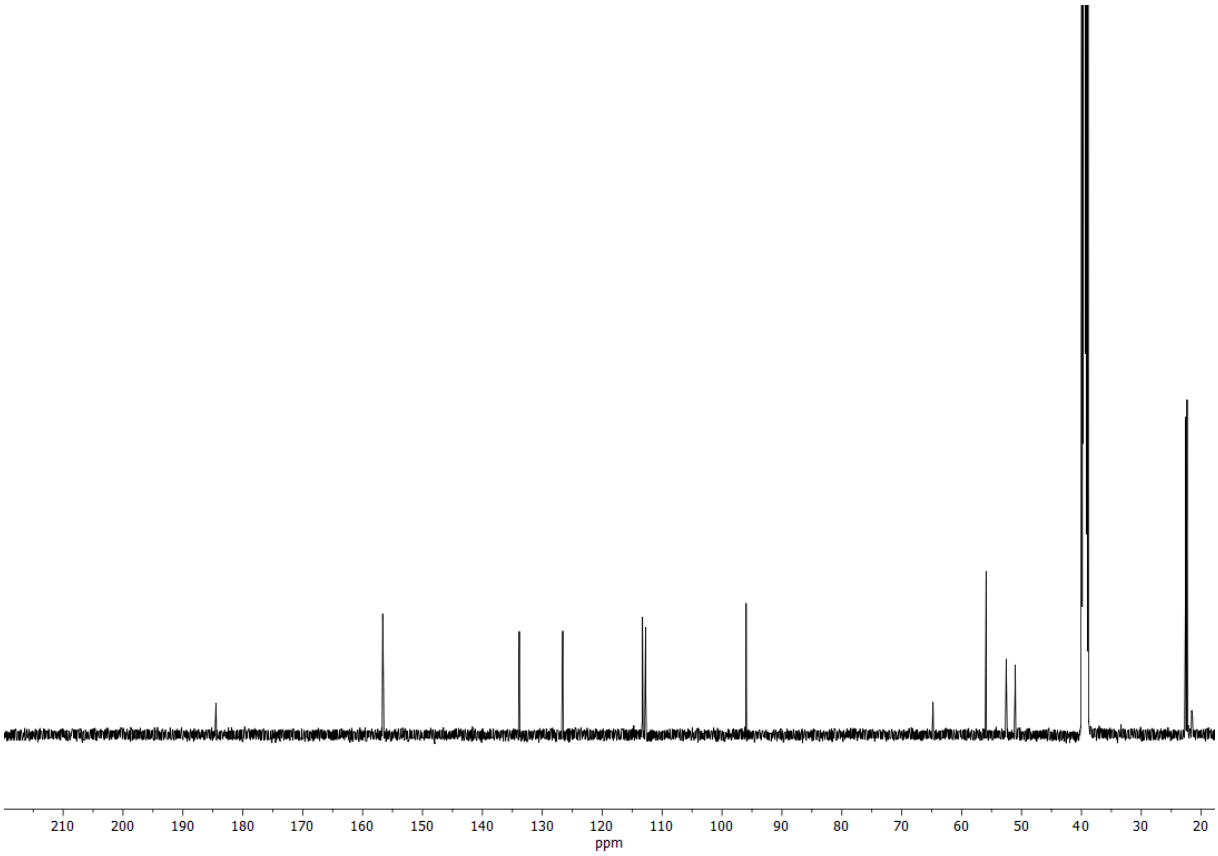

Figure S23: **Ag-4b**, ^{13}C NMR (DMSO, 126 MHz): 184.8 (ArC2), 156.5 (ArC5), 133.8 + 126.5 (ArC3 + ArC8), 113.18 (ArC), 112.62 (ArC), 95.92 (ArC), 55.81 (OCH_3), 52.46 (CH), 51.07 (CH), 22.53 (CH_3), 22.37 (CH_3).